GEOPHYSICAL RESEARCH LETTERS, VOL. 22, NO. 12, PAGES 1501-1504, JUNE 15, 1995

Contrail formation: Homogeneous nucleation of H_2SO_4/H_2O droplets

B. Kärcher,[1] Th. Peter,[2] R. Ottmann [3]

Abstract. Homogeneous nucleation of sub–nanometer H_2SO_4/H_2O germs, their growth and freezing probability in the cooling wake of a subsonic jet aircraft at tropopause altitude are investigated. Heteromolecular condensation, water uptake, and coagulation cause a small subset of the germs to grow into nm–sized solution droplets which overcome the Kelvin barrier. These droplets efficiently take up water vapor from the gas phase, dilute rapidly, and may eventually freeze as water ice. However, results discussed for the case of a B 747 airliner suggest that under threshold conditions for the onset of contrail formation, a visible contrail is not likely to be produced by this mechanism. The sensitivity of the calculations to uncertainties in the nucleation theory underlines the need for detailed measurements of the particle microphysics in young aircraft plumes.

Introduction

Contrails and the meteorological threshold conditions for their formation by jet aircraft are of key interest for a judgment of the chemical and climatological influence of air traffic on the atmosphere. *Appleman* [1953] derived a criterion by assuming water saturation as a necessary condition for contrail formation. The possibility of binary H_2SO_4/H_2O nucleation in aircraft plumes resulting from the emission of fuel sulfur and its subsequent oxidation to sulfuric acid has been suggested by *Hofmann and Rosen* [1978]. This hypothesis was recently supported by measurements by *Frenzel and Arnold* [1994] who showed that high levels of gaseous H_2SO_4 are produced in young plumes, and further supported by *Hagen et al.* [1994] who found both partially and totally soluble particles in the plume of cruising airliners consistent with particles resulting from binary nucleation. *Cooper and Nelson* [1994] evaluated the observed formation behaviour of 198 contrails and suggested that contrails are possibly initiated by the freezing of solution droplets formed from the soluble components of exhaust particles. Nucleation of H_2SO_4/H_2O droplets and their subsequent freezing is therefore a probable mechanism for ice particle formation in contrails which is energetically favored over direct water or ice nucleation because of the reduced water vapor pressure of the acidic solution. However, whether the solution droplets themselves are formed homogeneously or heterogeneously on soot particles is as yet unclear.

Previously, calculations of homogeneous H_2SO_4/H_2O nucleation rates in the wake of a jet aircraft have been published by *Miake-Lye et al.* [1994]. They did not address the subsequent growth of the droplets. The present paper presents a detailed model suited to describe the formation of ice particles by the freezing of aqueous sulfuric acid droplets which nucleate homogeneously in an aircraft plume. Our analysis also includes the SO_2 oxidation chemistry in the initial plume. We discuss our results for the case of a contrail generated by a B 747 airliner cruising at tropopause altitude under conditions which are marginally too warm according to the Appleman criterion, in order to investigate the possiblity of contrail formation by freezing of *in situ* produced solution droplets below the water saturation threshold. We perform an error analysis, describe modifications of the results due to radial mixing, and discuss the uncertainties in the classical nucleation theory for aircraft plume conditions.

Plume evolution and oxidation of SO_2

We describe the plume evolution using a trajectory box model which covers the jet, vortex, and dispersion regimes shown in Fig.1. We confine our study to an air parcel which is initialized at the exit plane of a single nozzle and then moves along the jet axis while expanding and cooling isobarically due to the entrain-

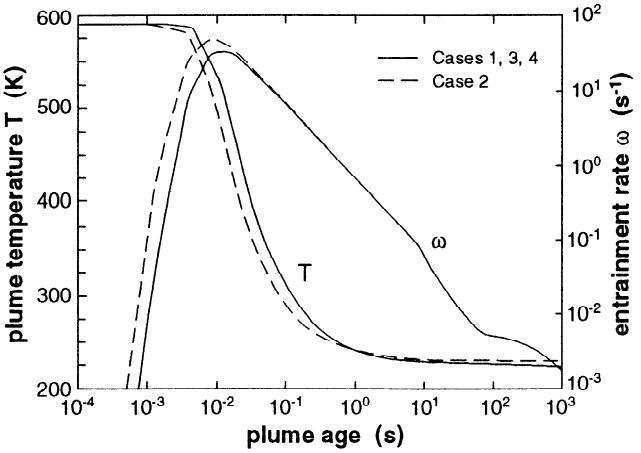

Figure 1. Plume temperatures and respective entrainment rates versus time as experienced by an air parcel that starts in the middle of the B 747 nozzle exit plane.

[1] Universität München, Freising.
[2] MPI für Chemie, Mainz.
[3] MPI für Extraterrestrische Physik, Garching.

Paper number 95GL01337
0094-8534/95/95GL-01337$03.00

ment of cold air. We assume the B 747 flies close to the tropopause at 240 hPa, at an ambient temperature of $T_a = 224$ K and a relative humidity of 63%. The plume never becomes supersaturated relative to water in our calculation (the maximum transient relative humidity is 95% at a plume age of 4 s). For this reference case (hereafter denoted by 1), we use emission indices of 0.72 g SO_2 and 0.16 g OH per kg fuel. To analyze the stability of our results against pertubations of the key parameters, we also present calculations with a faster cooling rate and enhanced value $T_a = 228$ K to keep the plume just below water saturation (case 2) and, alternatively, with an increased level of initial SO_2 ($\times$ 8.3) as case 3. The latter corresponds to 3 g S / kg fuel which is the internationally accepted maximum sulfur content for kerosene. As a data survey from 9 German fuel suppliers showed, the SO_2 emission index used in case 1 represents a typical value, whereas that of case 3 is much less representative for standard kerosene (R. Busen and U. Schumann, DLR, pers. communication). Finally, case 4 is identical with the reference case 1, but with $\pm 10\%$ variations of the surface energy σ of the solution droplets; droplet nucleation and growth rates are strongly nonlinear functions of σ.

The jet entrainment rates for temperature and species abundances have been extracted from a hydrodynamical fluid code that takes into account radial jet mixing [*Kärcher and Fabian*, 1994; *Kärcher*, 1994]. The corresponding rates in the vortex and dispersion regimes rely on simple parameterizations and are less important for the present discussion. As long as entrainment is weak (for plume ages $t < 0.01$ s), the temperature stays at its initial value of 590 K, then turbulent mixing causes the temperature to decrease rapidly, see Fig.1 (solid lines). At later stages, the mixing rate steadily decreases and the temperature slowly approaches the ambient value. In case 2 (dashed lines), cooling is markedly faster due to enhanced mixing. We note that the species entrainment rate is unchanged in all cases.

Figure 2 shows the number densities of OH, H_2O, and the sulfur species as a function of time. The hydroxyl radical is depleted primarily due to reactions with NO, NO_2, CO, and with itself on a timescale of a few ms. Consequently, only a small fraction of SO_2 can be oxidized by OH. The resulting SO_3, in turn, reacts rapidly with water vapor to H_2SO_4. We apply the mechanism proposed by *Stockwell and Calvert* [1983] for the gas phase conversion of SO_2 into H_2SO_4 *via* HSO_3 (not shown) and SO_3. Around $t = 20$ ms, the concentration of H_2SO_4 exhibits a maximum, corresponding to conversion rates around 0.5% of the total emitted SO_2 into H_2SO_4. This is in agreement with inferences from measurements [*Reiner and Arnold*, 1993] as well as more complex calculations [*Miake-Lye et al.*, 1994]. The oxidation of SO_2 ceases just before the entrainment significantly affects the chemistry, and this makes SO_2 behave like a tracer, asymptotically approaching its ambient abundance. The fate of H_2SO_4 is dominated by entrainment only in the time window 20 ms up to ~ 0.5 s. Later it diminishes much more rapidly, with additional depletion due to the onset of binary homogeneous nucleation (indicated by the arrow in Fig.2). Whereas faster cooling (case 2) merely leads to an earlier onset of depletion, a higher SO_2 exit plane abundance (case 3) results in a markedly faster removal of the gaseous H_2SO_4 reservoir. Note that an increase of the initial OH abundance (6 ppm in all cases) would lead to the same effect as an increase of SO_2, but the OH self-reactions limit the OH influence above ~ 10 ppm.

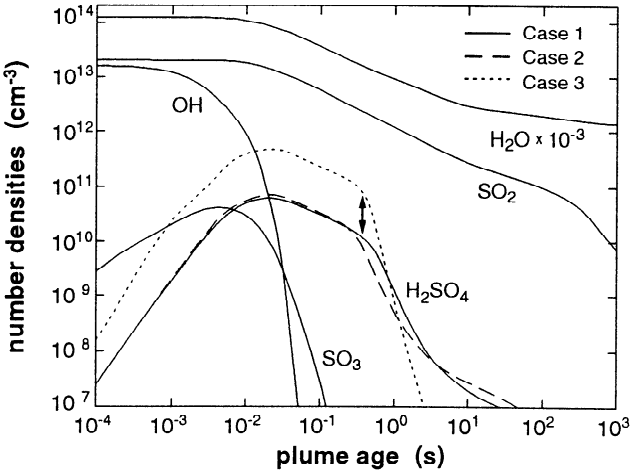

Figure 2. Temporal evolution of H_2O, OH, and the abundances of the sulfur species. The arrow indicates the depletion of H_2SO_4 due to binary nucleation.

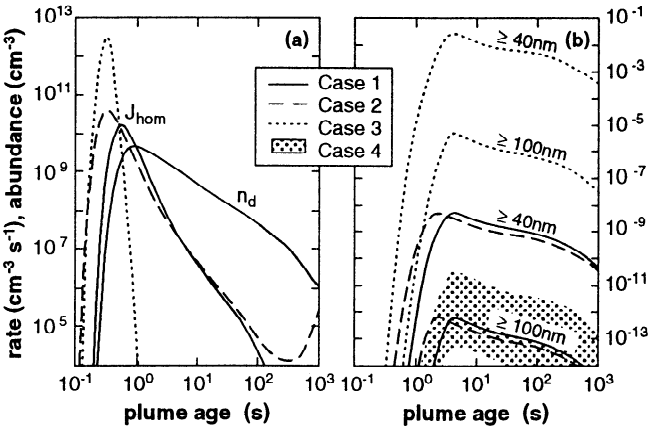

Figure 3. Homogeneous H_2SO_4/H_2O nucleation rates and droplet number density (a) and cumulative number densities of droplets with radii $r \geq 40$ nm and $r \geq 100$ nm (b) versus time.

Nucleation and freezing of droplets

We apply the classical heteromolecular nucleation theory as outlined by *Mirabel and Jaecker-Voirol* [1988] and employ thermodynamic relations given by *Gmitro and Vermeulen* [1964] together with solution vapor pressures based on the work of *Giauque et al.* [1959] with corrections discussed by *Hamill et al.* [1982]. Figure 3a shows homogeneous nucleation rates J_{hom} for the model cases 1,2,3 together with the total number density n_d of the nucleated solution droplets (case 1 only)

as a function of plume age. The steep rise of $J_{\rm hom}$ due to rapid cooling leads to a depletion of gaseous H_2SO_4 as seen in Fig.2. The nucleation rates are higher in cases 2 and 3 (most pronounced for the high H_2SO_4 levels reached in case 3) and the onset occurs slightly earlier than in case 1. After reaching its maximum, the droplet abundance n_d decreases rapidly due to coagulation. (Coagulation is calculated using the method proposed by *Toon et al.* [1988].) The timescales for both gas–to–particle conversion and coagulation are of similar magnitude (~ 0.5 s) and the corresponding microphysical processes are strongly coupled. Typical germ radii are $r_g = 0.4$ nm, with 1.5 sulfuric acid and 3 water molecules per germ on average. The small number of droplets that nucleate at a very early stage are slightly larger, because the supersaturation s is still low and $r_g \propto 1/\ln(s+1)$. As the temperature and H_2O abundance decrease, the droplets adjust to equilibrium conditions by rapid water uptake. Simultaneously, condensation onto the droplets is controlled by the impingement rate of H_2SO_4 molecules. This is the primary growth mechanism of the freshly nucleated droplets dominating water uptake and coagulation until the H_2SO_4 vapor becomes depleted. The results are sensitive to the strong dependence on $J_{\rm hom}$, and we try to keep effects of numerical diffusion in the growth equation small by choosing a moderately progressive increase of the radial bin sizes.

The homogeneous freezing rate $J_{\rm hom}^{\rm frz}$ [*Jensen et al.*, 1991; *Luo et al.*, 1994] of the exhaust–induced droplets is an extremely sensitive function of the H_2SO_4 weight fraction W and the temperature T. Figure 4 presents the temperature–composition diagram for the binary system H_2SO_4/H_2O for the cases 1,3,4. The thin solid lines are the melting point curves for ice and several hydrates of H_2SO_4. The W–T–histories of droplets in the plume with radii 0.4, 1, 4, and ≥ 100 nm are shown as thick solid lines and the right ordinate marks the corresponding plume age. The freshly nucleated droplets have H_2SO_4 weight fractions ranging from $0.7-0.8$, depending on germ radius. Figure 4 clearly reveals that, because of the Kelvin barrier, larger droplets condense and dilute markedly faster than smaller ones. For the total simulation time (10^3 s), the small droplets with $r \lesssim 2$ nm stay highly acidic and end up as supercooled liquid with weight fractions $W > 0.4$ after experiencing a growth and shrink cycle. (In case 2, evaporation of small droplets at $t = 400$ s causes the transient increase of $J_{\rm hom}$ as seen in Fig.3a.) In contrast, the droplets with $r \geq 4$ nm enter the freezing region within $1-2$ s after emission, see Fig.4. However, only the droplets with radii $r \geq 100$ nm experience homogeneous freezing rates $J_{\rm hom}^{\rm frz} = 10^{15}$ cm^{-3}s^{-1} (per unit droplet volume per second) around $t = 4$ s (cases 1,3, and 4) and $t = 2.5$ s (case 2), leading to reasonably short freezing timescales $\tau_{\rm frz} = 3/(4\pi r^3 J_{\rm hom}^{\rm frz}) \leq 0.25$ s. For $n_d(r \geq 40\,{\rm nm})$, it follows $\tau_{\rm frz} \leq 40$ s. From Fig.3b we infer that in all cases the number densities of droplets with radii $r \geq 40$ nm and $r \geq 100$ nm remain insignificant during the total simulation time. The net effect of faster cooling is merely to shift the concentration maxima (and the maximum relative humidity) from 4 s to 2.5 s; the enhanced nucleation rate in case 2 is compensated by an earlier depletion of gaseous H_2SO_4 and the higher final temperature, both slowing down the droplet growth rates. We observe similar compensation effects by varying the surface energy of the droplets (case 4). The smooth changes of the abundances due to variations of the droplet surface energy within the range $\pm 10\%$ are also depicted in Fig.3b (shaded region). In contrast, the high initial level of SO_2 (case 3) leads to both higher nucleation and growth rates and, in turn, to a more pronounced population of large particles. However, this effect is also limited by the fast removal of gaseous H_2SO_4 which rapidly cuts off the nucleation processes and hampers further growth of the droplets. Even though the droplets with $r \geq 40$ nm reach number densities up to 0.03 cm^{-3}, their freezing rates remain too small to make up a visible contrail. We note that contrail formation is observed in case 1 for ambient temperatures below 222 K, i.e., slightly below the Appleman threshold, when the largest droplets freeze as ice crystals and grow rapidly by depleting the water vapor. We point out that an accurate prediction of the time past exit when a contrail first becomes visible would require a full two–dimensional description. Calculations of $J_{\rm hom}$ in the radial flow field suggest a much earlier onset of nucleation (around 0.2 s) at 1–2 nozzle diameters off the jet axis, with comparable values for $J_{\rm hom}$ and somewhat less gaseous H_2SO_4. Thus, we expect that whether or not a visible contrail is formed is not affected by these geometrical considerations.

Finally we should like to stress that the classical theory of homogeneous nucleation we have applied is subject to considerable uncertainties. First, there is a size

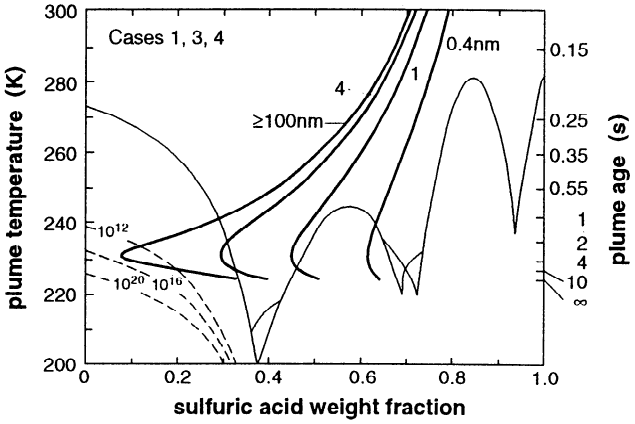

Figure 4. H_2SO_4 weight fractions of solution droplets with different radii (thick solid curves) as they evolve with temperature (left axis) and corresponding plume age (right axis). The dashed contour lines below the ice–liquid coexistence curve mark homogeneous freezing rates per unit droplet volume per second (cm^{-3} s^{-1}). The thin solid curves represent the melting point lines for ice and several H_2SO_4 hydrates. Only larger droplets overcome the Kelvin barrier and subsequently enter the freezing region.

effect because of the small discrete number of molecules in the sub–nanometer embryos (see, e.g., *Laaksonen and Kulmala* [1991]). This effect is in addition to the well–known weakness of the theory to rely on bulk phase properties [*Pruppacher and Klett*, 1978; p.168]. Second, the assumed steady–state of the embryo distribution could be violated under the rapidly changing, turbulent conditions in the plume. Third, the formation of gaseous, subcritical H_2SO_4/H_2O clusters can considerably affect the nucleation rates [e.g., *Mirabel and Jaecker–Voirol*, 1988], but we have no knowledge on the abundance of such clusters under plume conditions. Clearly, further theoretical research on these topics constrained by detailed experimental investigation of plume microphysics is needed.

Conclusions

Using a box model designed for microphysical investigations of jet aircraft plumes, we conclude that (1) the operation of jet aircraft has a great potential for releasing large amounts of volatile sulfuric aerosol into the atmosphere, even under conditions where no contrails are expected, and (2) binary homogeneous nucleation of H_2SO_4/H_2O is not likely to account for sufficient ice particle production under conditions close to the formation threshold temperature. The results proved to be stable under variation of the key parameters. The model predicts contrail formation by this mechanism only if the plume becomes water supersaturated during cooling. In such cases, homogeneous freezing of H_2SO_4/H_2O droplets will compete with possible other processes that lead to ice formation. In this regard, the nucleation properties of soot particles under plume conditions need to be investigated.

Acknowledgments. We wish to thank B.P. Luo who provided thermodynamic data and acknowledge fruitful discussions with D. Baumgardner, P. Mirabel, and W. Stockwell. This study was supported, in part, by the German Secretary of Education and Research.

References

Appleman, H., The formation of exhaust contrails by jet aircraft, *Bull. Am. Meteorol. Soc.*, *34*(1), 14–20, 1953.

Cooper, W. A., and L. D. Nelson, Threshold conditions for the formation of contrails, (to be published) 1995.

Frenzel, A., and F. Arnold, Sulfuric acid cluster ion formation by jet engines: Implications for sulfuric acid formation and nucleation, in *DLR–Mitteilung 94–06*, pp. 106–112, DLR/Köln, 1994.

Giauque, W. F., E. W. Hornung, J. E. Kunzler, and T. R. Rubin, The thermodynamic properties of aqueous sulfuric acid solutions and hydrates from 15 to 300° K, *J. Am. Chem. Soc.*, *82*, 62–70, 1960.

Gmitro, J. I., and T. Vermeulen, Vapor–liquid equilibria for aqueous sulfuric acid, *A. I. Ch. E. J.*, *10*, 740–746, 1964.

Hagen, D. E., P. D. Whitefield, and M. B. Trueblood, Particulate characterization in the near field of commercial transport aircraft exhaust plumes using UMR–MASS, in *DLR–Mitteilung 94–06*, pp. 119–124, DLR/Köln, 1994.

Hamill, P., R. P. Turco, C. S. Kiang, O. B. Toon, and R. C. Whitten, An analysis of various nucleation mechanisms for sulfate particles in the stratosphere, *J. Aerosol Sci.*, *13*(6), 561–585, 1982.

Hofmann, D. J., and J. M. Rosen, Balloon observations of a particle layer injected by stratospheric aircraft at 23 km, *Geophys. Res. Lett.*, *5*, 511–514, 1978.

Jensen, E., O. B. Toon, and P. Hamill, Homogeneous freezing nucleation of stratospheric solution droplets, *Geophys. Res. Lett.*, *18*(10), 1857–1860, 1991.

Kärcher, B., Transport of exhaust products in the near trail of a jet engine under atmospheric conditions, *J. Geophys. Res.*, *99*(D7), 14509–14517, 1994.

Kärcher, B., and P. Fabian, Dynamics of aircraft exhaust plumes in the jet regime, *Ann. Geophysicae*, *12*(10), 911–919, 1994.

Laaksonen, A., and M. Kulmala, Homogeneous heteromolecular nucleation of sulfuric acid and water vapors in stratospheric conditions: A theoretical study of the effect of hydrate interaction, *J. Aerosol Sci.*, *22*(6), 779–787, 1991.

Luo, B. P., T. Peter, and P. J. Crutzen, Freezing of stratospheric aerosol droplets, *Geophys. Res. Lett.*, *21*(13), 1447–1450, 1994.

Miake-Lye, R. C., R. C. Brown, M. R. Anderson, and C. E. Kolb, Calculations of condensation and chemistry in an aircraft contrail, in *DLR–Mitteilung 94–06*, pp. 274–279, DLR/Köln, 1994.

Mirabel, P. J., and A. Jaecker-Voirol, *Binary Homogeneous Nucleation, in: Atmospheric Aerosols and Nucleation*, vol. 309 of *Lecture Notes in Physics*, chap. 1, pp. 3–14, Springer–Verlag, Berlin, 1988.

Pruppacher, H. R., and J. D. Klett, *Microphysics of Clouds and Precipitation*, D. Reidel Publishing Comp., Dordrecht, Holland, 1978.

Reiner, T., and F. Arnold, Laboratory flow reactor measurements of the reaction $SO_3 + H_2O + M \rightarrow H_2SO_4 + M$, *Geophys. Res. Lett.*, *20*(23), 2659–2662, 1993.

Stockwell, W. R., and J. G. Calvert, The mechanism of the HO–SO_2 reaction, *Atmos. Environ.*, *17*, 2231–2235, 1983.

Toon, O. B., R. P. Turco, D. Westphal, R. Malone, and M. S. Liu, A multidimensional model for aerosols: Description of computational analogs, *J. Atmos. Sci.*, *45*(15), 2123–2143, 1988.

Bernd Kärcher, Universität München, Hohenbachernstr. 22, D–85354 Freising, FRG. Thomas Peter, MPI für Chemie, D–55020 Mainz, FRG. Renate Ottmann, MPI für Extraterrestrische Physik, D–85748 Garching, FRG.

(Received November 9, 1994; revised February 6, 1995; accepted March 17, 1995.)